

Molecular Organization in the Sarcoplasmic Reticulum Membrane studied by X-ray Diffraction

Y. DUPONT, S. C. HARRISON* & W. HASSELBACH

Max-Planck-Institut für medizinische Forschung, Abteilungen Biophysik und Physiologie, 69 Heidelberg 1

Orientated preparations of rabbit sarcoplasmic reticulum vesicles give X-ray diffraction maxima to a resolution of 16 Å. The calculated electron density profile shows that protein is distributed very asymmetrically in the membrane.

THE membrane system of the sarcoplasmic reticulum (SR) regulates the contractile cycle of muscle filaments by the uptake and release of calcium ions¹⁻³. Closed vesicles derived from the SR have been isolated in good yield from muscle homogenates and shown to concentrate Ca²⁺, using ATP as an energy source, in conditions similar to those prevailing *in vivo*⁴. The vesicles contain protein and lipid, in a ratio of about 65:35 (ref. 5). Several groups have shown that a major protein component, approximately 100,000 in molecular weight, accounts for a fraction of the total protein variously estimated as 30 to 60%⁶⁻⁸. The isolated protein possesses Ca²⁺-stimulated ATPase activity^{6,9}.

Electron microscopy of SR membranes reveals that the preparations contain vesicles ranging in diameter from 500 to several thousand angstroms¹⁰. Vesicles negatively stained

with uranyl acetate and phosphotungstic acid (PTA) appear to show an outer layer of 30-40 Å "spikes" or "particles" projecting from the membrane surface, and freeze-etched preparations have somewhat larger (80 Å) particles in the plane of cleavage¹¹. At least part of the ATPase molecule must be accessible from the exterior of the vesicle, as shown by ferritin active-site label experiments¹⁰. To define in greater detail the geometry of the SR membrane, we have prepared orientated specimens for X-ray diffraction. Our results show a distinct asymmetry in the organization of the SR membrane.

Orientated SR Vesicles

SR vesicles were prepared from rabbit skeletal muscle by standard methods^{12,13}. We introduced an additional purification just before preparation of the X-ray specimen by centrifuging through a discontinuous sucrose gradient (Spinco SW65 rotor, 25,000 r.p.m., 2 h). The largest fraction was consistently found in a band between sucrose solutions of density 1.11 g cm⁻³ and 1.13 g cm⁻³, and this fraction, dialysed against 0.02 M Tris-maleate, pH 7.2, 0.1 M KCl, 5% glycerol, was used for X-ray studies. Unfractionated vesicles gave identical diffraction patterns but with somewhat broader reflexions. Orientated specimens were obtained by centrifuging approximately 5 mg of SR (Spinco An-D rotor, 56,000 r.p.m., 12 h, 4° C) onto a mica strip, 1 mm × 12 mm, inserted into a 'Teflon' adapter at the bottom of a Beckman Model E analytical centrifuge cell. States of different water content were obtained by air-drying the 1 mm thick pellet in the cold for periods of up to 2 h. Coleman *et al.*¹⁴ used similar techniques for orientating SR and other membrane preparations.

The specimens were cooled during X-ray exposure, and no change of spacing was observed for periods of up to 4 d. Enzymatic activity of the preparation survived the orientation, partial drying, and X-ray exposure, as shown by the data in Table 1. Ca-stimulated ATPase assays showed 80 to 100% specific activity in re-homogenized samples that had been dried to give X-ray spacings between 190 and 265 Å. Moreover, Ca²⁺-uptake measurements indicated that a significant fraction of the re-homogenized vesicles were closed and capable of sequestering Ca²⁺.

An X-ray diffraction photograph of the SR membranes (Fig. 1) shows along the meridian orders of a single repeat whose spacing varies with the water content of the membranes. The diffraction generally extends to a resolution of 16 to 20 Å, depending on the state of the specimen. In many photographs we can detect traces of a meridional reflexion at about 60 Å, which becomes much stronger in very dry or maltreated samples. We attribute this line to an independent lipid phase, presumably from disrupted membranes. There are also rather diffuse equatorially orientated reflexions at 55 Å and in the 10 Å region. Our photographs are thus significantly better than those of Coleman *et al.*¹⁴ who obtained only a few orders from centrifuged, dried SR membranes.

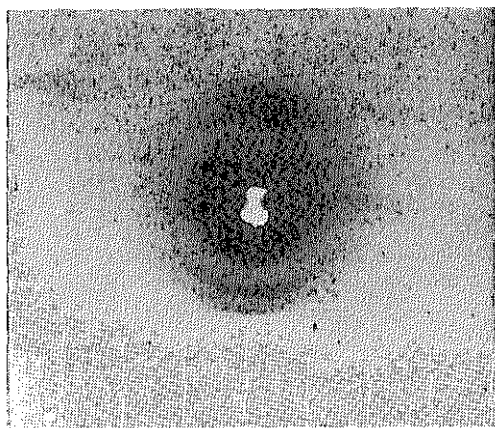


Fig. 1 X-ray diffraction photograph of orientated SR membranes. The second, third, fourth, sixth and seventh orders of a 234 Å repeat are visible. The orders 9, 11 and 13 can be seen on the original film. Equatorially orientated diffraction appears at 55 Å (just outside the position of the fourth meridional order). The photograph was taken with a mirror-monochromator point-focusing camera, used with an Elliott rotating-anode X-ray generator (focal spot 100 μm). The horizontal streaks are parasitic scatter from the quartz monochromator.

* Present address: Harvard University, Gibbs Laboratory 101, 12 Oxford Street, Cambridge, Massachusetts 02138.

Table 1 ATPase Activity and Rate of Ca^{2+} Uptake in SR Membranes after X-ray Exposure

	190 Å	X-ray spacing 240 Å	260 Å
ATPase	0.8	0.8	1.0
Ca-uptake	0.3	0.5	0.7

Activities are normalized to the measured activity (taken as 1.0) of an equivalent weight of fresh SR membranes, before preparation for X-ray experiment.

See ref. 8 for methods.

Spacing and Water Content

The meridional spacing varies continuously from 270 Å for a freshly packed specimen not subjected to drying (50% water by weight) to 170 Å for a rather dry specimen (25% water). We observed altogether more than fifteen different spacings. In one case we obtained eight different spacings by successive dryings of a single specimen, an experiment which permitted us to follow all the reflexions and to ensure that no reflexions from lipid phases were included in our measurements.

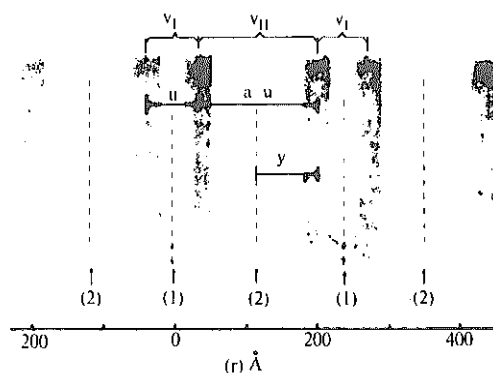


Fig. 2 Schematic diagram of packed vesicles. Considered in one-dimensional projection along the line perpendicular to the membrane planes, the distribution of matter has centres of symmetry between collapsed vesicles (2) and at the vesicle interior (1). The unit cell spacing is denoted by a and the two inter-membrane distances by u and $a-u$. The internal and external volumes v_I and v_{II} are shown to correspond to u and $a-u$, respectively. Evidence for this assignment is discussed in the text under the heading "Electron Density Profile." The scale at the bottom of the figure corresponds to a spacing $a=234$ Å.

The 170 to 270 Å repeat distance contains two apposed membranes; thus the line group of our one-dimensional unit cell has centres of symmetry. The shrinkage accompanying removal of water can in principle occur at either interface or at both—that is, at the vesicle interior or at the inter-vesicle surface (Fig. 2). Comparison of one-dimensional Patterson functions at different spacings indicates that over particular ranges of hydration, the shrinkage occurs in a relatively simple manner. The Patterson corresponding to a repeat distance $a=234$ Å appears in Fig. 3a. The peak at 37 Å remains essentially constant with spacing over the entire range; we attribute it to the inter-polar group vector (compare ref. 15). The strongest feature is the maximum at $u=68$ Å. If we ascribe this to a vector, u , between two membranes in a unit cell, then $a-u=166$ Å is the other inter-membrane distance (compare Fig. 2). Note that the separations u and $a-u$ are very unequal, suggesting a difference in the inside-outside distribution of mass. In Fig. 2, we have shown u as the vector across the interior of a single collapsed vesicle (volume v_I) and $a-u$ as the vector between vesicles (volume v_{II}). This assignment is at present arbitrary, but we indeed conclude below that there is more protein on the outer vesicle surface than on the inside

and that the longer vector ($a-u$) must extend across the interface of apposed vesicles.

The dependence of the distances u and $a-u$ on the spacing a is shown in Fig. 3b. In the "wet" range $220 < a < 270$, u varies more rapidly than $a-u$. In the "dry" range $170 < a < 220$, $a-u$ changes, while u remains constant. Within each range it should therefore be possible to trace a continuous transform by scaling diffracted amplitudes from specimens of different spacing. In the "dry" range this approach will depend on the assumption that no significant structural changes occur within the shrinking volume v_{II} , and in the "wet" range by the further assumption that the slower variation of v_{II} may be ignored in comparison with the shrinkage of v_I . We can evaluate these assumptions by analysing the continuous transforms themselves.

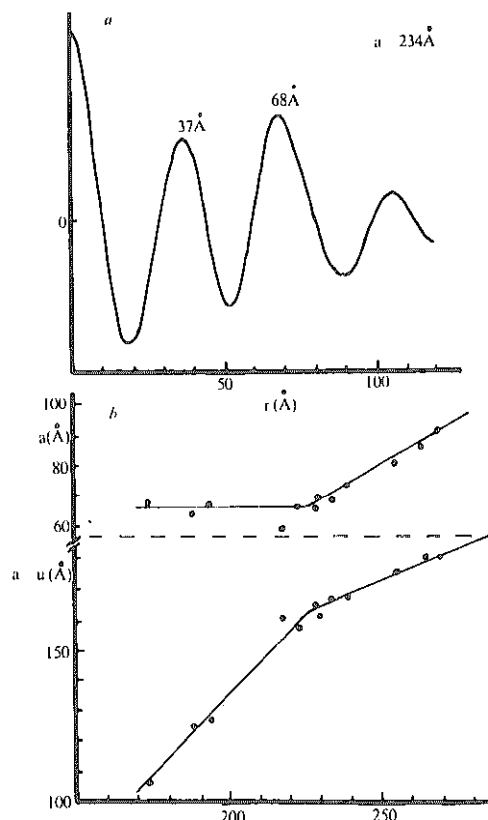


Fig. 3 *a*, One-dimensional Patterson function, calculated using intensities measured from the photograph in Fig. 1 ($a=234$ Å). The photograph was photometered with a small beam along the meridian, and the $F^2(h)$ were obtained from the area under each peak by applying a Lorentz factor proportional to h^2 (as for a powder pattern). The internal and external volumes V_I and V_{II} are shown to correspond to u and $a-u$ respectively. *b*, Dependence of u and $a-u$ on total spacing, a . See Fig. 2 for definitions.

The transforms are shown in Fig. 4. They consist of a series of alternating peaks and nodes. Within each peak, the signs of all terms must be the same. We can invoke the principle of minimum wavelength¹⁷ and conclude that the signs of the first three peaks of the dry transform and of the first six of the wet transform must alternate. The phases are thus determined to within an overall sign ambiguity to a resolution of about 30 Å. We have calculated Fourier syntheses to resolve this ambiguity; only one of the two sign sequences gives a plausible profile (Fig. 5). It is not possible to continue the phasing in this manner, however, due to the broad region of low amplitude in the continuous transform near 0.037 \AA^{-1} . That is, the signs of the fourth and fifth maxima in the dry transform or of the eighth, ninth and tenth in the wet transform are undetermined with respect to the low resolution terms.

Within the region $0.04 \text{ \AA}^{-1} < R < 0.06 \text{ \AA}^{-1}$ the minimum wavelength argument again applies: only an overall ambiguity of high-resolution signs with respect to low resolution signs remains unresolved. With available data, we are unable to make a choice between the two alternatives.

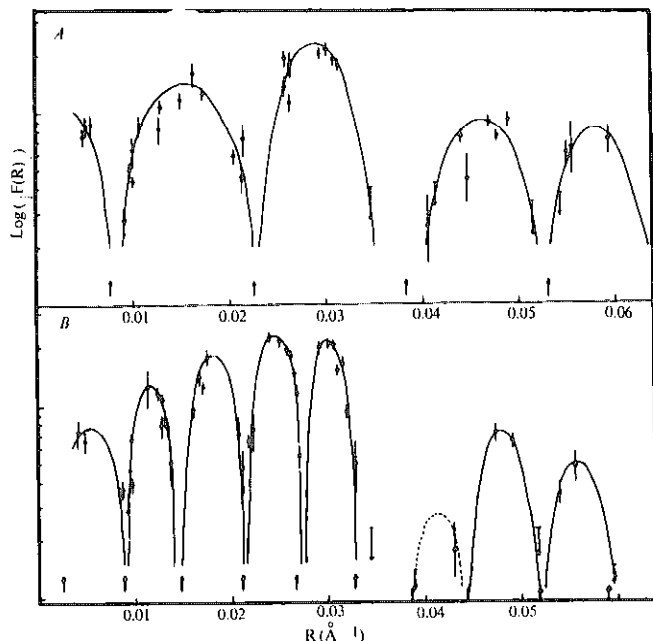


Fig. 4 Continuous transforms for SR membranes in wet and dry hydration ranges, derived by combining the corrected diffraction amplitudes corresponding to various spacings a . The data for different spacings were scaled by normalizing the sum $1/a \sum h^2 I(h)$ for all reflexions between 0 and $(30 \text{ \AA})^{-1}$. A, "Dry" transform: $190 \leq a \leq 234$. Arrows indicate nodes of $\cos 2\pi(34)R$; B, "wet" transform: $220 \leq a \leq 240$. Arrows indicate nodes of $\cos 2\pi(83)R$. We can understand the spacing of the nodes for each continuous transform by considering that the principal contrast in the electron-density variation across the membrane comes from the essentially centrosymmetric profile of a lipid bilayer, as in the treatment of the myelin structure by Caspar and Kirschner¹⁶. We do not need to introduce the assumption of a centrosymmetric bilayer into our analysis. We describe the continuous transforms in these terms here simply to make clearer the nature of their variation. Let $f(R)$ be the transform of this profile referred to an origin at its centre and let y and $(a-y)$ be the positions of the membrane centres in the unit cell (compare Fig. 2). Then the transform of the two-membrane structure, referred to the proper unit-cell origin, is $2f(R)\cos 2\pi yR$. In the "wet" range, it is appropriate to use centre of symmetry 2 (Fig. 2) as the origin, since we take v_{11} to be approximately constant. Then $y = 1/2(a-u) = 83 \text{ \AA}$ and the nodes of $\cos 2\pi yR$ are rather closely spaced, coinciding well with the nodes of the "wet" transform. In the "dry" range, v_1 is constant, and choosing centre of symmetry 1 (Fig. 2) as the origin, we obtain $y = 1/2 u = 34 \text{ \AA}$. Again, the nodes of the observed transform coincide approximately with the zeroes of $\cos 2\pi yR$.

Electron Density Profile

Figure 5 shows the distribution of electron density across the SR membrane, calculated from the unambiguously-phased low-resolution reflexions. The profiles for three different hydration states are given. Their similarity is consistent with the arguments presented above, that no major structural changes occur on mild dehydration, and it is indeed this similarity that has been the basis of our approach to determining the structure. An analogous method has been used in X-ray studies of myelin¹⁵, and the comparison of different lattices containing identical structures is also a useful technique in protein crystallography¹⁸.

An asymmetrically placed minimum is the most prominent feature of the SR electron density profile. It indicates a

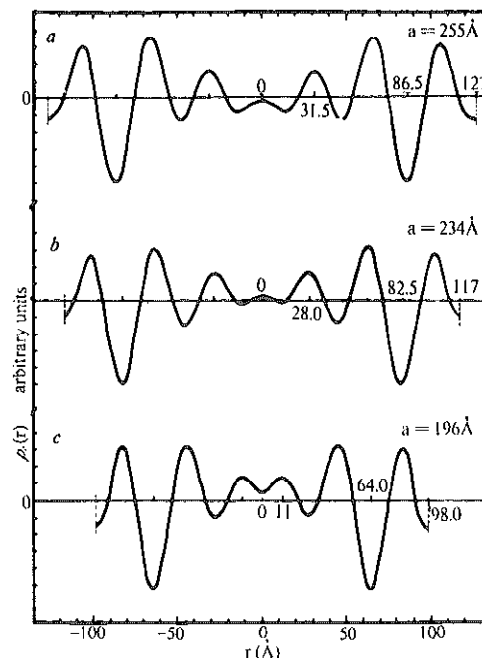


Fig. 5 Electron density distribution across the SR membrane. Density in arbitrary units is plotted as a function of the distance, r , across the membrane. The three profiles were computed to a resolution of 30 \AA using the unambiguously phased reflexions, with signs indicated below. a, $a = 255 \text{ \AA}$: $+0-+0-++$; b, $a = 234 \text{ \AA}$: $+-+--+-+$; c, $a = 196 \text{ \AA}$: $++-+-+--$.

bilayer organization of lipid in the membrane. The maxima to either side are spaced about 40 \AA from each other: they show the position of lipid polar groups and associated protein (compare the low resolution profile of myelin). A density maximum appears at about $50-55 \text{ \AA}$ from the bilayer centre. Its consistent appearance in all three profiles indicates that it is a significant feature, and not a Fourier cut-off effect. It must represent protein that projects from one side of the membrane, and we can probably identify it with the projections seen in electron micrographs of negatively stained vesicles¹¹. This interpretation determines the inside and outside of the vesicle in our profiles. It is presumably the projecting structure that gives rise to the large asymmetry in u and $a-u$ (Fig. 3b). The minimum inter-membrane distance observed on the external side with the projecting density maximum is about 110 \AA , whereas the membranes can approach on the internal side to a distance of 66 \AA .

SR Membrane Organization

We have demonstrated that there is in the SR membrane a strongly asymmetric distribution of protein about a lipid bilayer. The minimum in the electron density profile does not, however, imply that this bilayer be continuous. Indeed, the composition of the SR requires that some protein penetrate—or dip into—the lipid. We can see this by calculating the length fraction of the one-dimensional unit cell occupied by lipid. The data in Table 2 show that one lipid bilayer has an "equivalent thickness" of about 26 \AA . Since the distance between polar groups estimated from the electron density profile is about 40 \AA , the calculation implies that $30-40\%$ of the volume in the inter-polar group region contains either protein or water. A model with either partial or complete penetration by the ATPase protein is clearly the most plausible. The projections and the corresponding peak in the density profile could then represent either a tail of the ATPase molecule itself or a further protein component. The magnitude of the electron density maximum suggests that it includes about 20% of the total membrane protein. The reconstituted membranous structures obtained from purified ATPase show no projections¹⁹, but the organ-

ization of the reconstituted structure cannot at this stage be assumed identical to the native.

Table 2 Length Fractions of the Repeat Distance Occupied by Lipid, Protein and Water for Wet and Dry Orientated SR Vesicles

Spacing (a)	Water content (± 5%)	Length fraction		
		Lipid	Protein	Water
270 Å	50%	0.19	0.26	0.55
170	25%	0.30	0.41	0.29

The calculations are based on a protein : lipid ratio of 65 : 35 and on the water content determined by weighing a sample before and after drying over P₂O₅. We assumed mean densities of 1.0 and 1.37 for lipid and protein respectively.

Do our results provide constraints for describing the mechanism of Ca²⁺ transport in the SR? The fact that we can record discrete meridional reflexions out to 15 Å resolution indicates that there is a relatively high degree of order across the membrane. Moreover, the asymmetry of the structure is its most striking feature. The ATPase molecules must therefore adopt quite uniform orientations and positions with respect to the lipid bilayer. Isolation of the ATPase and restoration of activity by added lipid make it reasonable to assume that in the membrane this protein and associated lipid represent the entire functional transport unit^{9,19,20}. Since major translations or reorientations of the large ATPase proteins would require significant disruption of the asymmetric organization, our results favour a description of Ca²⁺ transport in which the transport system functions with at most relatively modest

conformation changes.

We thank Dr B. Agostini for taking electron micrographs of our specimens and Miss A. Migala for technical assistance.

Received February 20; revised April 20, 1973.

- ¹ Hasselbach, W., *Prog. Biophys. biophys. Chem.*, **14**, 169 (1964).
- ² Weber, A., in *Current Topics in Bioenergetics* (edit. by Sanadi, D. R.), **1**, 203 (Academic Press, New York, 1966).
- ³ Sandow, A., *A. Rev. Physiol.*, **32**, 87 (1970).
- ⁴ Hasselbach, W., and Makinose, M., *Biochem. Z.*, **333**, 518 (1961).
- ⁵ Fiehn, W., and Hasselbach, W., *Eur. J. Biochem.*, **13**, 510 (1970).
- ⁶ MacLennan, D. H., *J. biol. Chem.*, **245**, 4508 (1970).
- ⁷ MacFarland, B. H., and Inesi, G., *Arch. Biochem. Biophys.*, **145**, 456 (1971).
- ⁸ Hasselbach, W., in *Molecular Bioenergetics and Macromolecular Biochemistry*, 149 (Springer, New York, 1972).
- ⁹ Hasselbach, W., and Migala, A., *FEBS Lett.*, **26**, 20 (1972).
- ¹⁰ Hasselbach, W., and Elfvin, L.-G., *J. ultrastruct. Res.*, **17**, 598 (1967).
- ¹¹ Deamer, D. W., and Baskin, R. J., *J. Cell Biol.*, **42**, 296 (1969).
- ¹² Hasselbach, W., and Makinose, M., *Biochem. Z.*, **339**, 94 (1963).
- ¹³ de Meis, L., and Hasselbach, W., *J. biol. Chem.*, **246**, 4759 (1971).
- ¹⁴ Coleman, R., Finean, J. B., and Thompson, J. E., *Biochim. biophys. Acta*, **173**, 51 (1969).
- ¹⁵ Wilkins, M. H. F., Blaurock, A., and Engelman, D., *Nature new Biol.*, **230**, 72 (1971).
- ¹⁶ Caspar, D. L. D., and Kirschner, D. A., *Nature new Biol.*, **231**, 46 (1971).
- ¹⁷ Bragg, W. L., and Perutz, M. F., *Proc. R. Soc. Lond.*, **A**, **213**, 425 (1952).
- ¹⁸ Rossmann, M. (ed.), *The Molecular Replacement Method* (Gordon and Breach, New York, 1972).
- ¹⁹ MacLennan, D. H., Seeman, P., Iles, G. H., and Yip, C. C., *J. biol. Chem.*, **246**, 2702 (1971).
- ²⁰ Racker, E., *J. biol. Chem.*, **247**, 8198 (1972).